私立東海大學

資訊工程與科學研究所

碩士論文

指導教授：黃育仁 博士

3-D 能量都卜勒乳房超音波影像的血管化特徵

電腦輔助診斷之研究

Computer-aided Diagnosis for Breast Tumors by Using

Vasculization of 3-D Power Doppler Ultrasound

研究生：許嘉家

中 華 民 國 九 十 七 年 六 月

摘要

血管化是腫瘤產生、生長與擴散時公認的基本程序，腫瘤內血管化的程度與腫瘤的良惡性有絕對的相關性，許多已發表的研究使用彩色都卜勒超音波來估算乳房腫瘤的血管化特徵，結合彩色都卜勒超音波與傳統的灰階超音波影像能夠有效地定位腫瘤血管，並區分乳房腫瘤的良惡性，然而，彩色都卜勒超音波難以偵測到與主軸方向垂直的血管。近年來的研究指出，能量都卜勒超音波對血流偵測之敏感度較彩色都卜勒超音波高，且能量都卜勒超音波在血管角度、深度的影響與血管尺度限制較小，因此能量都卜勒超音波用於偵測乳房腫瘤的血管化特徵以及分類乳房腫瘤之良惡性上，都優於彩色都卜勒超音波。三維的能量都卜勒超音波影像較二維的超音波影像包含了更多的血流資訊，能夠偵測整個乳房腫瘤的血管化，且惡性腫瘤的體積通常較大，三維灰階超音波影像能夠估算出非常近似於真實乳房腫瘤的體積，可作為區分乳房腫瘤良惡性之有用的特徵。此外，一份統計的資料指出乳癌與病人的年齡有關，通常 40 歲以上的婦女得到乳癌的機率較高，因此，本論文提出一乳癌三維能量都卜勒超音波影像血流特徵電腦輔助診斷系統，利用從三維能量都卜勒超音波影像中所取得的腫瘤血流特徵，再加入腫瘤體積與病人年齡，來區分乳房腫瘤之良惡性。首先，請醫師針對三維灰階超音波影像上的乳房腫瘤繪出有興趣的區域(Volume of Interest, VOI)，依照此區域計算近似於真實腫瘤大小的體積，接著估算三維能量都卜勒超音波中的血流特徵，再加入病人的年齡形成特徵向量，最後使用支援向量機(Support Vector Machine,

SVM)來分類乳房腫瘤。支援向量機的學習速度快且較穩定，能夠減少訓練的時間並得到良好的分類結果，大大的提升了診斷速度與正確性。實驗結果證明，本論文利用支援向量機，結合腫瘤血流、體積與病人年齡等特徵，來分類乳房腫瘤的良惡性，得到令人滿意的準確度。此外，本論文也使用等位函數法(Level set method)自動切割乳房腫瘤，使用自動切割所得到的輪廓區域去估算以上所提的特徵，並與原始方法比較診斷之結果。

關鍵字：3-D 能量都卜勒超音波影像，腫瘤血管化，乳房腫瘤，電腦輔助診斷系統，支援向量機，等位函數法

ABSTRACT

Rationale and Objectives: To evaluate the accuracy of three-dimensional (3-D) power Doppler ultrasound in differentiating benign and malignant breast tumors by using support vector machine (SVM).

Materials and Methods: 3-D power Doppler ultrasonography were obtained from 164 patients (age range, 17-80 years; mean age, 44 years) with 86 benign and 78 malignant breast tumors. The volume of interest (VOI) in 3-D ultrasound images was automatic generated by using three rectangular region of interest. The vascularization index (VI), flow index (FI) and vascularization-flow index (VFI) on 3-D power-Doppler ultrasound images were evaluated for the entire volume area, the computer extracted VOI area and the opposite area of VOI. Patients' age and the volume of VOI were also applied to identify breast tumors. Besides, this study also proposed an automatic contouring method by using level set method (LSM) to extract the similar 3-D volume and improve the diagnostic accuracy. The level set segmentation automatically extracted 3-D contours of breast tumors from ultrasound images after the image preprocessing. In this study, each ultrasonography classified as benign or malignant based on 11 features by using the SVM model. In the experiment, all the breast tumors were sampled with k-fold cross-validation (k = 10) to evaluate the performance with receiver operating characteristic (ROC) curve.

Results: The sensitivity, specificity, positive predictive value (PPV), negative predictive value (NPV) and accuracy of SVM for classifying malignancies were 94%, 67%, 72%, 92% and 80%, respectively. The classification performance in terms of A*z* value for the ROC curve of the features derived from 3-D power Doppler is 0.91. Comparing to this CAD system, the performance of the CAD system with automatic contouring method is better.

Conclusions: The vascular features of 3-D power Doppler ultrasound combined with patients' age and volume of VOI are effective in differentiating benign and malignant breast tumors by using SVM.

Keywords: three-dimensional power Doppler, tumor vascularity, volume of interest, computer-aided diagnosis, support vector machine, level set method

INDEX

LIST OF TABLES

LIST OF FIGURES

CHAPTER 1

INTRODUCTION

Tumor vascularity has proved to be an important factor that correlated with tumor malignancy[1,2]. Angiogenesis is widely accepted as a fundamental process for the establishment, growth and dissemination of all tumors. The growth of breast cancer is connected to angiogenesis during the development of the tumor. Comparing to benign tumors, breast cancers are expected to display increased vascularity[3]. Various investigations reported the vascularity of the breast tumors and distinguish between benign and malignant lesions by using color Doppler ultrasound[4-6]. Color Doppler sonography characterizes blood flow velocities and the calculation of resistance indices by using the mean Doppler frequency shift at a particular position. The heterogeneous vascularity of breast malignancies is the major problem in flow assessment with color Doppler[7]. The vessels perpendicular to the bean direction are poorly detected by the color Doppler. A study designed for preoperative assessment of a breast lesion showed that color Doppler sonography was not superior to other diagnostic methods due to color Doppler can be affected when the direction of the probe changes[8].

Power Doppler was developed to improve the visualization of small vessels by using a different measurement of the strength of the Doppler signal which fundamentally depends on the amount of blood. Power Doppler ultrasound can be used

to detect the course of tumor vessels more clearly due to power Doppler is less angle-dependent and not velocity-dependent. Thus power Doppler imaging was better in classification of benign and malignant breast masses than conventional color Doppler imaging on the basis of assessment of tumor vascularity[9,10]. These studies have proved that power Doppler ultrasound have a higher diagnostic accuracy than in color Doppler ultrasound. In particular, three-dimensional (3-D) power Doppler ultrasound can quantify the power Doppler signal and detect the total vascularity within the entire volume of breast tumor[11,12].

Besides, the volume information of a breast tumor is also important for physicians to make diagnostic decisions. Extracting the tumor volume from the 3-D ultrasound was very similar to the real size of tumor. Due to malignant tumors frequently have a large size, the volume data of breast tumor has been considered as a useful characteristic for differentiating between benign and malignant breast tumors[13-15]. Moreover, recent interest in patients' age is associated with breast cancer[15]. A statistics have showed that the breast cancer usually occur at a woman over 40 years old[16]. The patients' age is positively related to likelihood that a tumor is malignant.

The aim of this paper is developing a computer-aided diagnosis (CAD) for power Doppler imaging to assist physicians in diagnosis and improves the prevision accuracy. This study classified each breast tumor as benign or malignant by using support vector

machine (SVM). The SVM model has become extremely popular in terms of classification and prediction[17-19]. This technique having outstanding and speedy classification ability was applied extensively to not only classification but also image recognition and bioinformatics[20-23]. In this study, vascular features, tumor volume and patients' age were considered as features to difference benign and malignant breast tumors. The SVM model was employed as a classifier to evaluate the capability of 3-D power Doppler ultrasonographic technology for the differential diagnosis of solid breast tumors.

In chapter 2, a CAD system for 3-D power Doppler imaging was proposed. The vascular features, patients' age and volume of VOI were applied to distinguish between benign and malignant tumors by using SVM. Moreover, this study designed an automatic contouring method for the proposed CAD system in chapter 3. The proposed CAD system classified breast tumors by evaluating vascular features and volumes of tumors from the automatic 3-D contours. The classification performance by using SVM of the CAD system with automatic contouring was compared with the CAD system without that. It is concluded from the experiment that combined 3-D power Doppler vascularity with patients' age and tumor size has a good result of difference benign and malignant breast tumors.

CHAPTER 2

COMPUTER-AIDED DIAGNOSIS

2.1 DATA ACQUISITION

There were pathologically proved 86 benign and 78 malignant breast tumors in 164 patients whose ages ranged from 17 to 80 years (mean age, 44 years) in this study and it was approved by the institutional review board and ethics committee at Changhua Christian Hospital. All of the 3-D ultrasound imaging and 3-D power Doppler ultrasound imaging was performed with a scanner (Voluson730, GE Healthcare, Zipf, Austria, equipped with RSP 6-12 transducer) and a transducer. The transducer was a linear-array broadband probe with a frequency of 6 to 12 MHz, has a scan width of 37.5 mm and a sweep angle of 5 to 29 to obtain 3-D volume scanning. A preinstalled 20° sweep angle and power Doppler settings with mid frequency, 0.9 kHz pulse repetition frequency, -0.6 gain, and “low 1” wall motion filter were fixed for all women in this study. Both the operator and patient hold breath around 20 seconds as possible during the scanner generate the 3-D volume.

The image database containing 164 3-D volumes in 164 patients were collected from January 2003 to December 2003. Each 3-D volume had 199 2-D ultrasound images with corresponding power Doppler ultrasound images. Figure 1 presents the ultrasound image and its corresponding power Doppler ultrasound image.

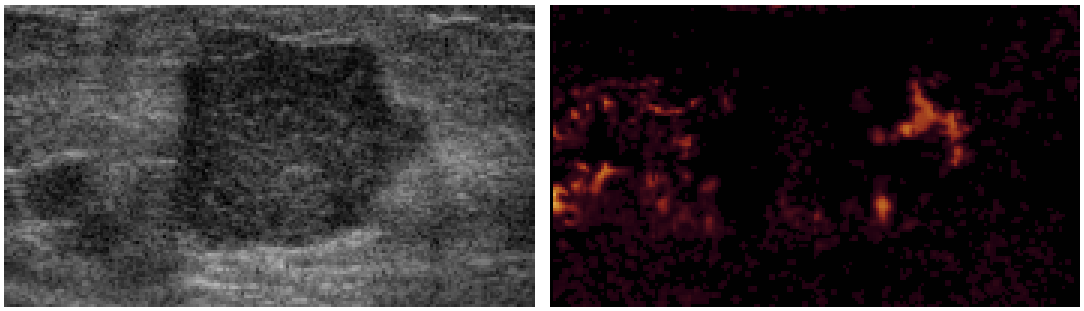

(a) (b)

Fig. 1. (a) The ultrasound image of a malignant tumor, and (b) its corresponding ultrasound power Doppler imaging.

2.2 VOI EXTRACTION

To extract the volume of interest (VOI) in 3-D ultrasound imaging, a physician with experience in breast ultrasound examination defined and manually selected rectangular region of interest (ROI) including the tumor border in the specific three slices, i.e. the first, middle and last slices in 3-D ultrasound imaging[24]. The first, middle, and last slices were the slice with appeared tumor, the largest diameter of the tumor and the tumor is tending to disappear, respectively. Figure 2 illustrates an example of the ROI for the three slices that manually selected by the physician. After the ROI regions in the three slices were defined, the VOI area would be extracted from the 3-D volume. Figure 3 presents generation of the VOI area in a 3-D power Doppler ultrasound imaging.

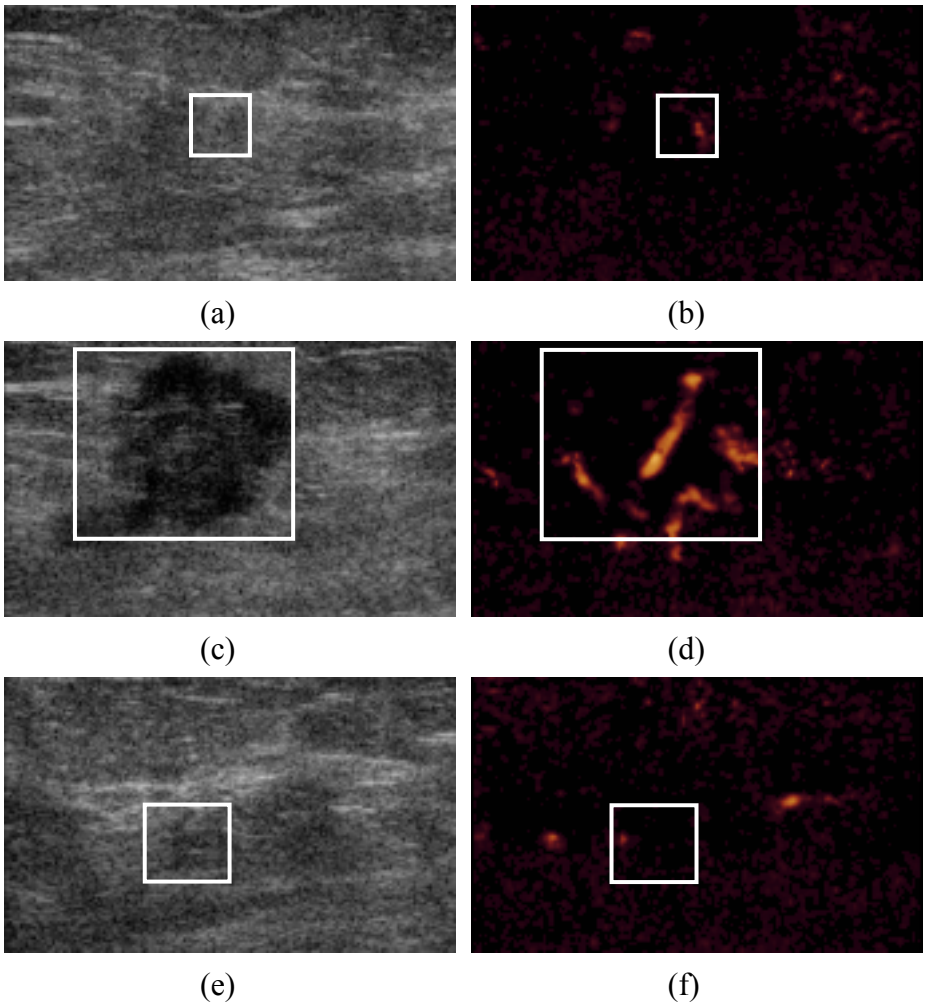

Fig. 2. Physician manual selected ROI (white rectangle) of specific slice for B-mode ultrasound and power Doppler ultrasound: (a)-(b) the first slice with corresponding power Doppler image slice, (c)-(d) the middle slice with corresponding power Doppler image slice, and (e)-(f) the last slice with corresponding power Doppler image slice.

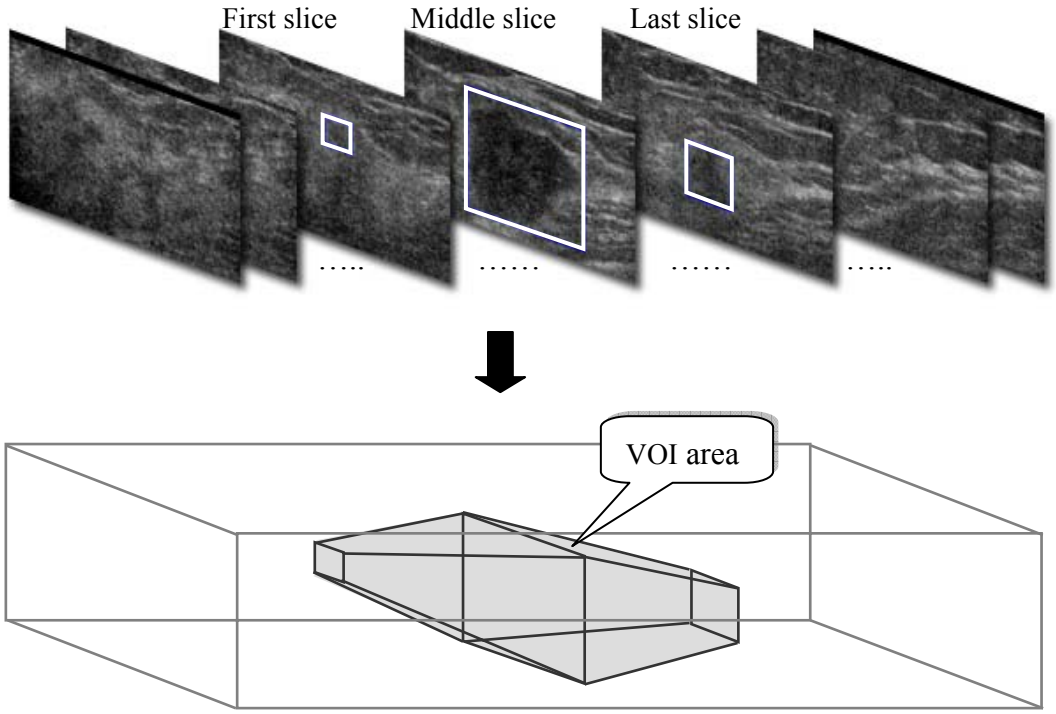

Fig. 3. The 3-D volume of interest (VOI) area in a 3-D ultrasound imaging.

2.3 FEATURE EXTRACTION

To quantify the power Doppler signal, three indices were evaluated from 3-D power Doppler ultrasound, i.e. vascularization index, flow index and vascularization flow index[25]. Vascularization index (denoted *VI*), the ratio between the color voxels (with power Doppler signal) and the total number of voxels in the region of interest, represents the vessel in the tissue. Let *S* denoted the set of all slices in a 3-D power Doppler ultrasound imaging, the *VI* is defined as

$$VI = \frac{\sum_{s \in S} P(s)}{\sum_{s \in S} N(s)}, \tag{1}$$

where $P(s)$ is the number of pixels with power Doppler signal and $N(s)$ is the number of total pixels in the specific area of the slice s. Flow index (denoted FI), the mean energy per color voxel, represents the average intensity of flow. The FI is defined as

$$FI = \frac{\sum_{s \in S} I(s)}{\sum_{s \in S} P(s)}, \tag{2}$$

where $I(s)$ is the intensity sum of pixels with power Doppler signal in the specific area of the slice s. Vascularization flow index (denoted VFI), the mean color value in all the voxels in the obtained volume, represents both vascularization and flow. The VFI for the specific area of the slice s is defined as

$$VFI = \frac{\sum_{s \in S} I(s)}{\sum_{s \in S} N(s)}. \tag{3}$$

This study calculated the three indices from the entire volume area, the computer extracted VOI area and the opposite area of VOI. Figure 4 shows the specific voxel areas in a 3-D power Doppler imaging. The vascularization indices VI_{VOI}, VI_E and VI_O were estimated by using the VOI area, the entire volume area and the opposite area, respectively. The flow indices FI_{VOI} (flow index from the computer extracted VOI area), FI_E (flow index from the entire volume area) and FI_O (flow index from the opposite area

of VOI) were estimated. For the vascularization flow indices, the VFI_{VOI}, VFI_E and VFI_O were by the corresponding area in the 3-D power Doppler imaging. Eventually, this study gained nine vascularization indices for the areas surrounding the breast lesion after image analysis. In addition to vascular features, patients' age and the volume of VOI (mm^3) are used to encode features for the SVM classifier.

2.4 SUPPORT VECTOR CLASSIFICATION

Support vector machines (SVMs) are machine learning methods based on the statistical learning theory and can be applied to classification[17,26]. It is able to extract the relevant discriminatory information form the training data. The aim of SVM is to generate a classification function from a set of training data and classify data into two classes. SVM maps the training data to a higher dimensional feature space and construct a maximal separating hyperplane. The separating hyperplane maximizes the distance between two parallel hyperplanes that separates the data on each side of the hyperplane. Figure 5 shows an optimal separating hyperplane with the largest distance between two parallel hyperplanes, and the data points belongs to two classes.

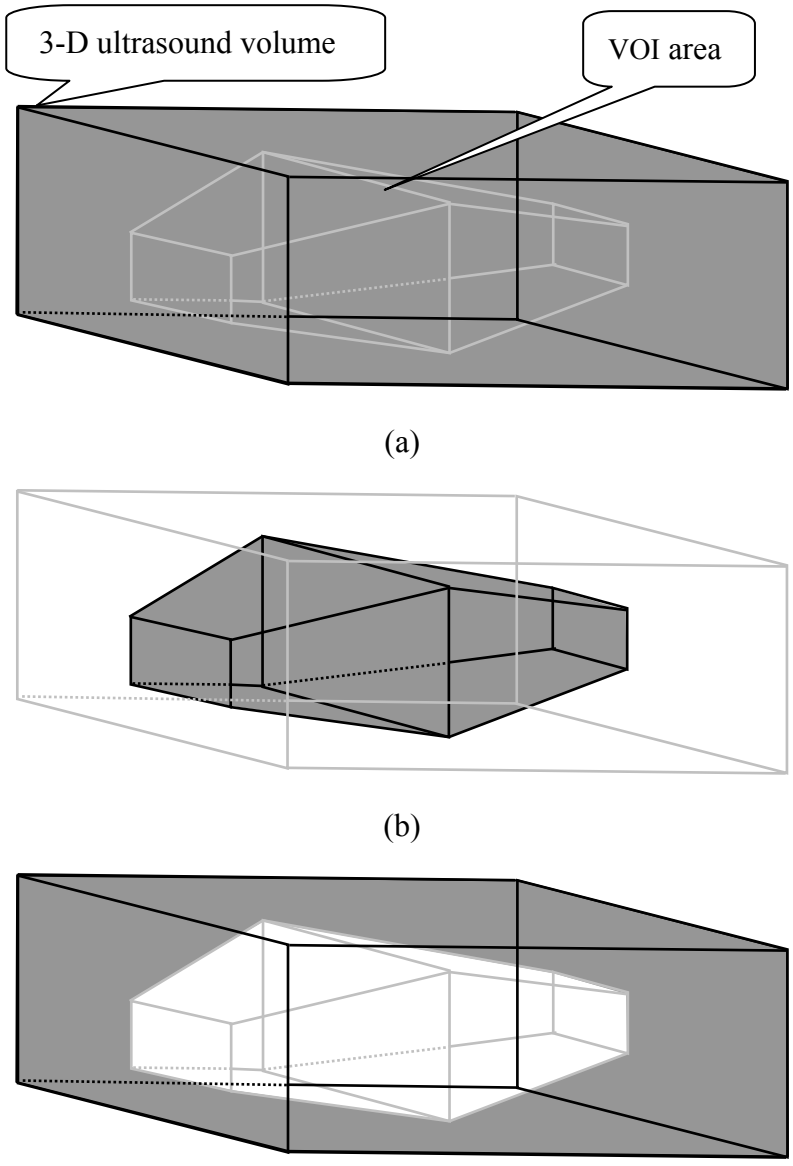

Fig. 4. The areas (colored gray) used for computing VI, FI and VFI indices for a 3-D power Doppler imaging: (a) the entire volume, (b) the extracted VOI and (c) the opposite zone of VOI.

Given a set of training vectors with a total of m vectors, (x_1, y_1), (x_2, y_2), (x_3, y_3), …, (x_m, y_m), where $x_i \in R^d$ denotes the value of i^{th} input vector and the y_i is either 1 or -1.

Let (x_i, y_i) is the corresponding desired output. The SVM distinguish the correct classification by means of the optimal separating hyperplane with the maximal margin, which takes the form

$$wx + b = 0, \tag{4}$$

then try to maximize the distance between two parallel hyperplanes that separates the data points on each side. The input vectors must be satisfied

$$y_l = wx_l + b \geq 1, \tag{5}$$

$$y_l = wx_l + b \leq -1, \tag{6}$$

these can be rewritten as

$$y_l(wx_l + b) \geq 1. \tag{7}$$

The support hyperplanes denote the hyperplanes that separate the data points on each side. And the data points lying on support hyperplanes are support vectors. The classification solution is given by the decision function

$$f(x) = sign\left(\sum_{i=1}^{n} \alpha_i y_i k(s_i, x) + b\right), \tag{8}$$

where α_i is the positive Lagrange multiplier, s_i are the support vectors (n in total), and $k(s_i, x)$ is the function for convolution of the kernel of the decision function. The support vector is the same class with $y = 1$ when $f(x) \geq 0$ and $y = -1$ when $f(x) < 0$. The radial kernels performs best in our experimental comparison, hence is chosen in the proposed diagnosis system. The radial kernels is defined as

$$k(x,y)=\exp\left(-\gamma(x-y)^2\right), \tag{9}$$

where $\gamma \in R$ is a non-zero parameter.

In this study, we classified each breast tumor as benign or malignant by using SVM. A total of 11 features including vascular features, patients' age, and volume of VOI from a breast tumor formed a feature vector, which was then utilized as the input vectors for the SVM classifier. The maximal separating hyperplane separates the positive values from the negative values. This study classifies the tumor has positive output value as malignant and negative output value as benign.

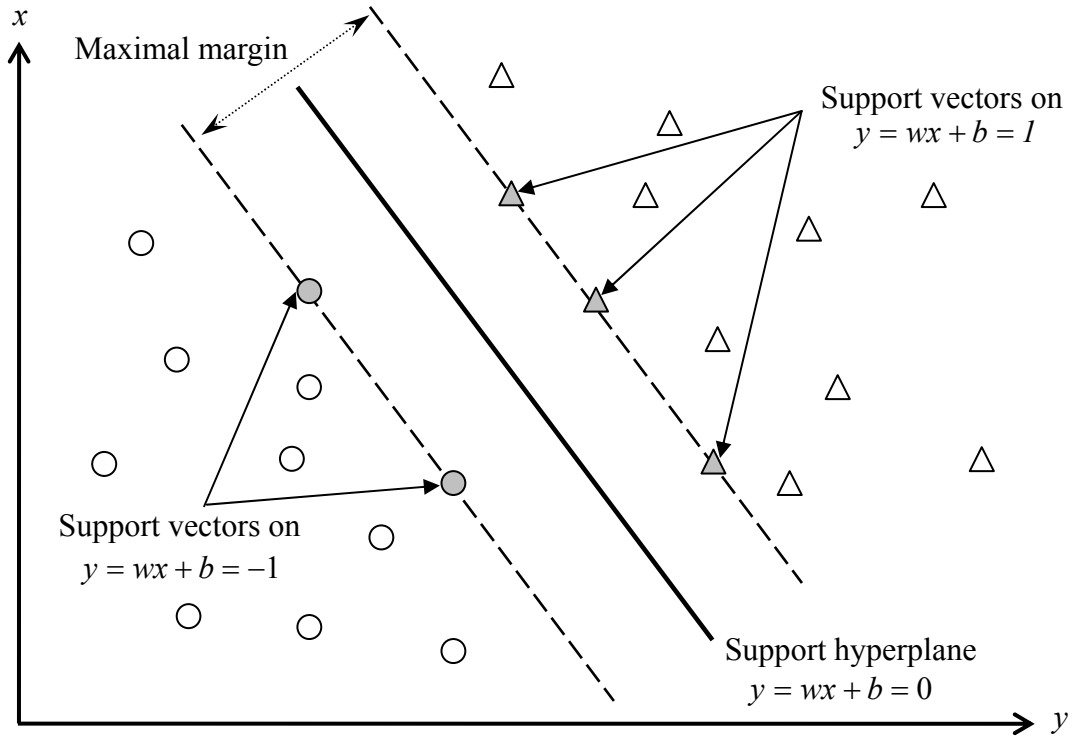

Fig. 5. The optimal separating hyperplane of support vector machine (SVM) with the maximal margin between two parallel hyperplanes.

2.5 RESULTS

The sonography database contained 164 pathologically proven cases (86 benign and 78 malignant barest tumors). To evaluate the performance, this study randomly divided all cases into *k* groups by the k-fold cross-validation method. The first group was used as a test group and the other (*k*-1) groups are used to train the SVM. To repeat this process until all *k* groups have been taken turns as the group used for testing. In the experiment, *k* was 10 and each group has 16 or 17 cases. The radial kernels of SVM obtaining the best result were chosen in this study. In the simulations, different γ values of radial kernels for the SVM system were performed to evaluate the classification performance. With the γ ranged from 0.001 to 0.002, the SVM model used in this work obtained a stable and the highest accuracy.

The classification results by the proposed CAD were showed in table 1. The accuracy of SVM for classifying malignancy in this study was 80% (131/164), the sensitivity was 94% (73/78), the specificity was 67% (58/86), the positive predictive value (PPV) was 72% (73/101), and the negative predictive value (NPV) was 92% (58/63). At the receiver operating characteristic (ROC) analysis, the classification performance of the SVM system was examined by the index of the area (A*z*) under the ROC curve. Table 2 lists the A*z* values and standard deviations of the 11 features. Figure 6 presents the ROC curves of the propose method in this study and the A*z* value was

0.91. From this result, combining vascular features of 3-D power Doppler ultrasonography with patients' age and volume of VOI were effective in differentiating benign and malignant breast tumors by using SVM.

Table 1. Classification of breast nodules by support vector machine (SVM) model.

	Benign*	Malignant*
SVM output < 0	TN 58	FN 5
SVM output ≥ 0	FP 28	TP 73
Total	86	78

*Histological finding

TN: The number of benign case which are diagnosed correctly.
FP: The number of benign cases which are misdiagnosed.
TP: The number of malignant cases which are diagnosed correctly.
FN: The number of malignant cases which are misdiagnosed.

All analyses were made on a single CPU Intel Pentium-VI 2.4 GHz personal computer (ASUSTek Computer Inc., Taipei, Taiwan) with Microsoft Windows XP® operating system. The programs were performed using C++ language and complied using the Microsoft Visual Studio®. The C++ codes were performed using Matlab software (The MathWorks, Inc., Natick, MA).

Table 2. The A*z* values and standard deviations of the 11 features including vascular features, patients' age, and volume of VOI.

Feature	A*z*	std
VI_E	0.7407	0.0406
VI_{VOI}	0.6714	0.0431
VI_O	0.7658	0.0386
FI_E	0.6980	0.0406
FI_{VOI}	0.6416	0.0428
FI_O	0.6931	0.0407
VFI_E	0.7733	0.0390
VFI_{VOI}	0.6789	0.0428
VFI_O	0.7760	0.0387
Volume of VOI	0.8138	0.0328
Patients' age	0.7940	0.0344

std: standard deviation

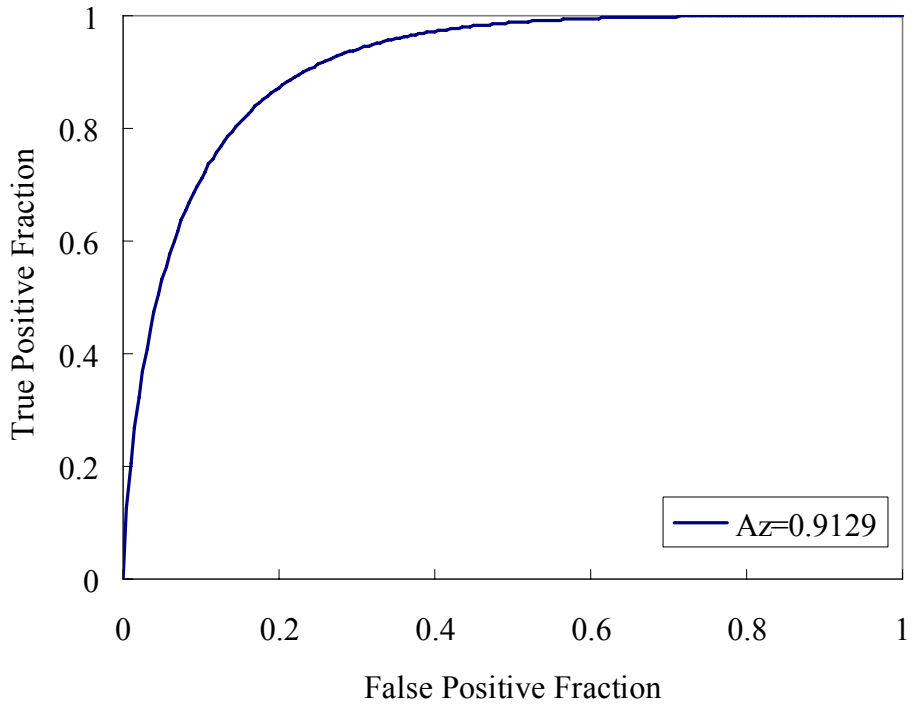

Fig. 6. Receiver operating characteristic (ROC) analysis of the proposed computer-aided diagnosis (CAD) system with the entire feature sets.

CHAPTER 3

AUTOMATIC CONTOURING METHOD

To improve the performance of VOI extraction in the proposed CAD system, an automatic contouring method for breast tumors in 3-D ultrasound imaging is necessary. A similar 3-D contour of a breast tumor can evaluate the more precise size of the tumor and the more precise vascularization indices in inner and outer tumor of corresponding 3-D power Doppler ultrasound. Due to the 3-D volume of a tumor is essentially constructed by a sequence of 2-D images in this study, the method for finding contours of a tumor should be extended to 3-D cases. Then the volume of tumor can be extracted by precisely counting the volume from the 3-D images. This chapter presented an efficient method for automatically detecting 3-D contours of breast tumors in 3-D ultrasound images.

The proposed contouring method included two stages. In the first stage, a preprocessing filter contained Wiener filter and Gaussian filter were utilized to reduce the any amount of noises but preserves the shape and contrast of breast tumor. The second stage, the ROI area including the border of the tumor with the largest diameter from the middle slice was manually selected by the physician and was used to be the initial contour. The deformation-based level set segmentation automatically extracted precise contour of breast tumor from the middle slice. The automatically extracted

contour of the tumor in the middle slice was used to be the initial contour for the tumor in the preceding slice and following slice. Then, the level set segmentation automatically extracted the contours and each extracted contour was used to be an initial contour for the tumor in the next preceding slice or following slice. Finally, after all the contours in ultrasound image slices were defined, the 3-D volume of tumor would be extracted from the 3-D ultrasound image.

The proposed CAD system with automatic contouring method evaluated 3-D volumes from the image database which was used in the previous CAD system. The vascular features and volume of tumor were calculated from the 3-D contour and were utilized combined with patients' age as the input feature vectors for the SVM classifier. The diagnostic performance was evaluated with receiver operating characteristic (ROC) curve and compared with the previous CAD system.

3.1 IMAGE PREPROCESSING

Due to the medical ultrasound B-mode images include considerable noises, speckles and tissue textures that make segmentation difficult. Image preprocessing is a significant issue before the segmentation. The aim of an effective preprocessing method for contouring is to reduce noises and preserve the useful information, such as edge and boundary of tumors. The Wiener filter which was proposed by Norbert Wiener is one of the tools of choice in removing noise from images[27][28]. The purpose of Wiener filter

is to reduce the amount of noise present in a signal by comparison with an estimation of the desired noiseless signal. The Wiener filter, based on statistical approach, is commonly referred to as the minimum mean square error filter or the least square error filter.

The goal of the Wiener method is to filter out noise that has corrupted a signal. The Wiener low-pass filter estimates the local mean and variance around each pixel,

$$\mu = \frac{1}{NM} \sum_{n_1, n_2 \in \eta} a(n_1, n_2), \tag{10}$$

$$\sigma^2 = \frac{1}{NM} \sum_{n_1, n_2 \in \eta} a^2(n_1, n_2) - \mu^2, \tag{11}$$

where is the $N \times M$ local neighborhood of each pixel in the image A. The Wiener filter then creates pixel-wise estimations,

$$b(n_1, n_2) = \mu + \frac{\sigma^2 - \nu^2}{\sigma^2}(a(n_1, n_2) - \mu), \tag{12}$$

where ν^2 is the noise variance. If the noise variance is not given, The Wiener filter uses the average of all the local estimated variances.

This study performed the Wiener filter to reduce the amount of noise present in the breast ultrasound images. Beside, another common filter was performed to smooth the ultrasound images after the Wiener de-noising. The Gaussian low-pass filter was utilized to smooth images and remove detail and noise. Gaussian smoothing is often applied because the noise or the nature of the object observed might be of a Gaussian probable form. The use of the Gaussian kernel for smoothing has become extremely

popular. This has to do with certain properties of the Gaussian as well as several application areas such as edge finding and scale space analysis.

In the proposed method, two filters, Wiener filter using neighborhoods of size 3 × 3 and Gaussian low-pass filter with a parameter sigma = 2, were performed to reduce noises and make the contour finding easily. Figure 7 presents the de-nosed results by applying the Wiener filter and Gaussian low-pass filter. The proposed method utilizing the Wiener filter preprocessing not only reduced the number of speckles, the amount of noises and the number of tissue-related textures in ultrasound images but also preserved the shape and contrast of breast tumor. Then, in order to smooth the image and make the contour finding easily, the Gaussian low-pass filter was performed after the Wiener filter. After the ultrasound images are preprocessed, the suspected tumors will be extracted based on the following segmentation steps.

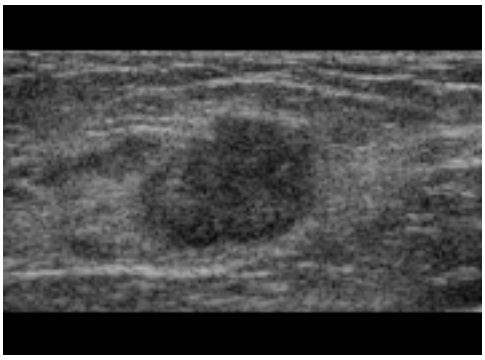

(a)

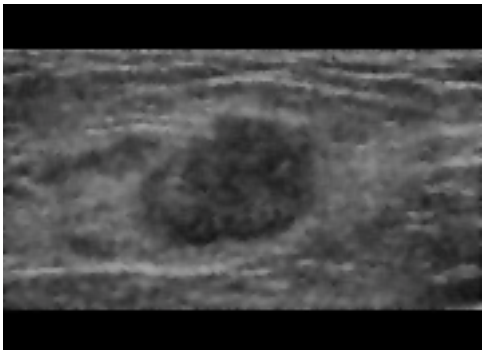

(b)

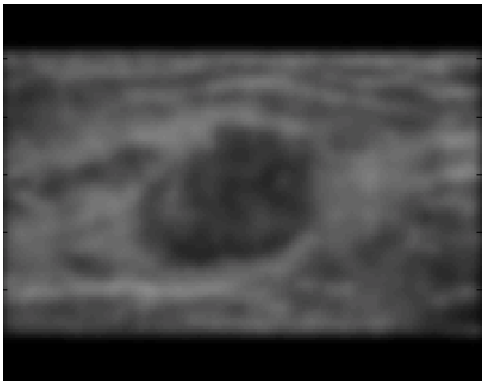

(c)

Fig. 7. Results of the image preprocessing: (a) the original ultrasound image, (b) through with Wiener filtering using neighborhoods of size 3 × 3, (c) through with Gaussian low-pass filtering with sigma = 2.

3.2 LEVEL SET CONTOURING

After the image preprocessing, an automatic contouring method was performed to segment the tumors in 3-D ultrasound imaging. The level set method is a numerical technique for analyzing the curve propagation and tracking interfaces moving under complex motions. This method offers a highly robust and accurate method and has been applied successfully to solve difficult problems of ultrasound image segmentation[29]. The level set method amounts to representing a closed curve Γ in the plane as the zero level set of an auxiliary function ϕ,

$$\Gamma(0)= \{x \mid \phi(x, t) = 0\}, \tag{13}$$

and then manipulating Γ implicitly, through the function ϕ. This function is called a level set function. ϕ is assumed to take positive values inside the region delimited by the curve Γ and negative values outside. The evolution equation of the level set function ϕ can be written in the following general form:

$$\frac{\partial \phi}{\partial t} + F \mid \nabla \phi \mid = 0 , \tag{14}$$

which is called level set equation with a given value of the initial function $\phi(x, t = 0)$. The function F is called the speed function. For image segmentation, the function F depends on the image data and the level set function ϕ. At any one point, the speed function F is based solely on the input intensity u_0[30]:

$$F = -\left(\alpha D(u_0) + (1-\alpha)\nabla \cdot \frac{\nabla \phi}{|\nabla \phi|} \right) \tag{15}$$

and

$$D(u_0) = \frac{(U-L)}{2} - \left(u_0 - \frac{(U+L)}{2} \right), \tag{16}$$

where α is a free curvature parameter that controls the degree of smoothness, U and L denote the adaptive maximal and minimal intensities in the subimage of the identified contour, respectively. Figures 8 show the surface propagation of an initial contour and the accompany movement of the function ϕ [29].

Due to the 3-D volume of a tumor is essentially constructed by a sequence of 2-D images in this study, the method for finding contours of a tumor should be extended to 3-D images. This proposed method can get the volume of tumor by precisely counting the volume of the 3-D images. In the proposed contouring method, the original ultrasound images were first processed by the Wiener filtering and Gaussian low-pass filtering. The ROI region which used to be the initial contour for the middle slice was manually selected by the physician. If the ROI region in the middle slice was too huge or very closing to the boundary of the image, the length and width of ROI would be reduced to be the initial contour. Because a huge initial contour and a contour which was very closing to the boundary of the image would make segmentation fail.

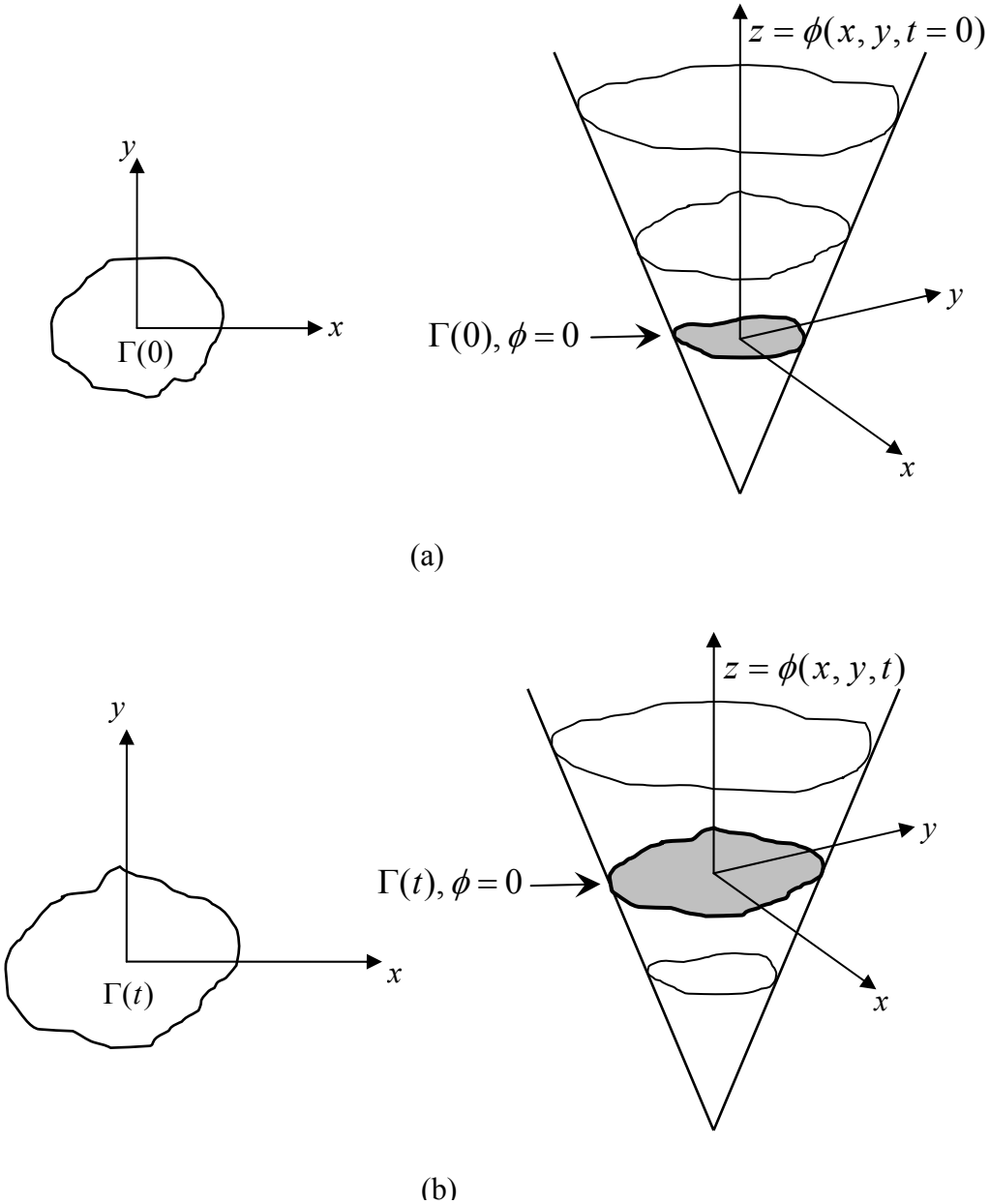

Fig. 8. Level set curve propagation: (a) the initial contour and the corresponding surface, (b) the contour and the corresponding surface at time *t*.

After extracting the initial contour from the middle slice, the level set method was performed to segment the tumor. The automatically extracted contour of the tumor in the middle slice was then used to be the initial contour for the preceding slice and

following slice. And the level set segmentation automatically extracted the contours from the tumor in the preceding and following slices. Then, each extracted contour is used to be an initial contour for the tumor in the next preceding slice or following slice. When the contour is disappearing or the tumor does not exist in the next image slice, the automatic contouring will stop. Finally, after all the contours of a tumor in ultrasound image slices were defined, the 3-D contour of tumor would be extracted from the 3-D ultrasound image.

Figure 9 presents a flowchart of the proposed method, in a form that includes the preprocessing and segmentation phases. After the 3-D contours of tumors were defined, the proposed CAD system can evaluate the similar volumes of breast tumors and the vascular features from the 3-D power Doppler ultrasound images. Then, the SVM will distinguish between benign and malignant tumors and the ROC analysis will be applied to evaluate diagnostic accuracy of the proposed CAD system with automatic contouring method.

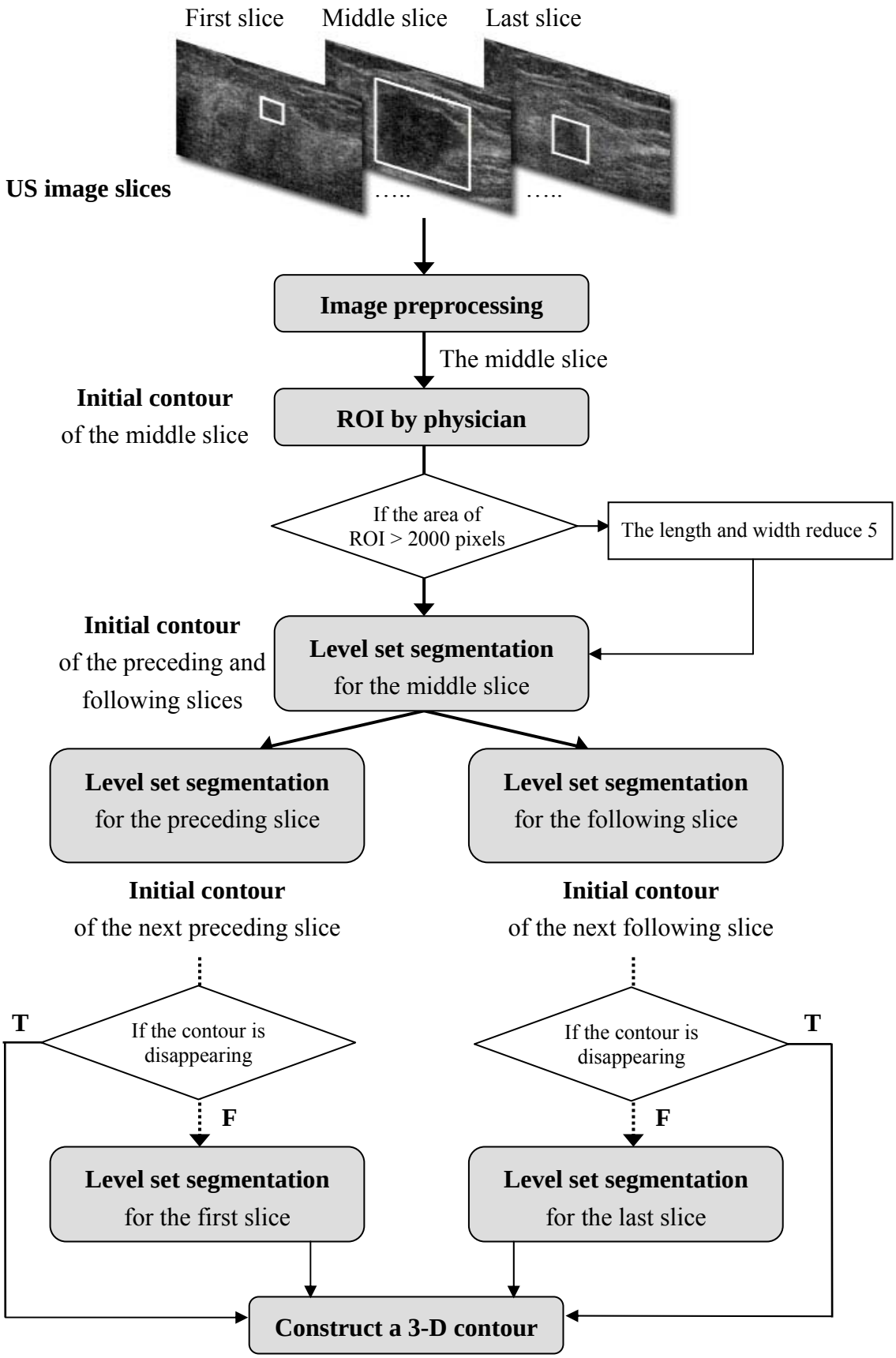

Fig. 9. The flowchart of the proposed contouring method.

3.3 DIGNOSTIC RESULTS

This study will show that the proposed CAD system with automatic contouring method have rather good performance and lead to a satisfactory result in comparison with the previous CAD system. Ten cases were excluded from the 3-D image database because the automatic segmentations of these tumors were failed. A total of 154 pathologically proved tumors were analyzed in this chapter. The vascular features and volume of tumor were calculated from the 3-D contour and were utilized combined with patients' age as the input feature vectors for the SVM classifier. The diagnostic performance was evaluated with receiver operating characteristic (ROC) curve. And the diagnostic accuracy of the CAD system with automatic contouring method was compared with the previous CAD system.

Figure 10(a)-(b) and figure10(c)-(d) show the contour evaluation for the middle slice in benign and malignant cases, respectively. Due to the ROI of the malignant tumor in figure 10(c) was huge and very closing to the boundary of the image, the length and width of the ROI was reduced 5 pixels. And the preceding slices and the following slices in a benign case are showed in figures 11(a)-(c) and figures 11(d)-(f), respectively. Figure 12 show the preceding slices and the following slices in a malignant case. The proposed method clearly yielded contour that are similarly to the real contour of the tumor. From the segmentation results, only a small number of cases were

unattainable; the tumors are too big to out of images or too small to make disappearance of contours.

In the experiment, the radial kernels and γ ranged from 0.001 to 0.002 of SVM were chosen in the proposed CAD system with contouring method. Comparing with the previous CAD system, the classification performance of both CAD systems were examined by the index of the area (Az) under the ROC curve. Table 3 lists the A*z* values and standard deviations of the 11 features in the proposed CAD system with contouring method and the previous CAD system. Figure 13 presents the ROC curves of the propose CAD system with contouring method and the previous CAD system in this study and the A*z* value was 0.91 and 0.9, respectively. The A*z* value in the proposed CAD system with contouring method was better than the previous CAD system. From this result, the proposed CAD system with contouring method was effective in differentiating benign and malignant breast tumors by using SVM.

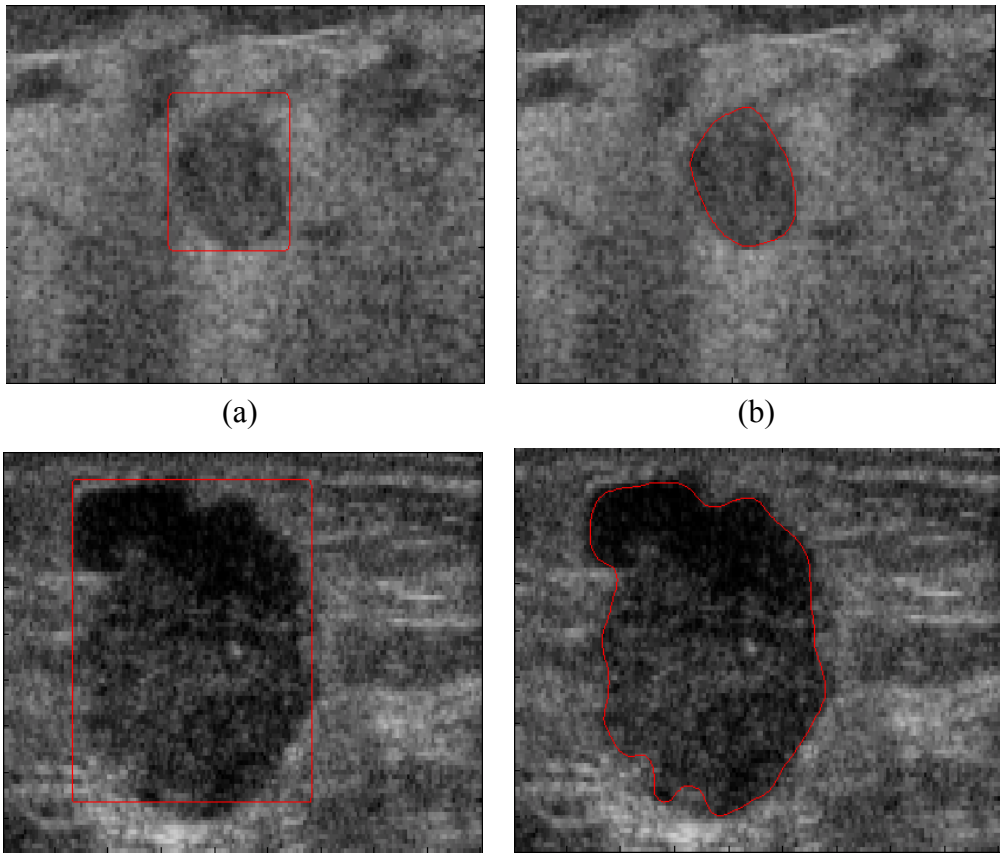

Fig. 10. Result of contour segmentation in the middle slice: (a)-(b) the initial contour and the extracted contour of segmentation of a benign case, and (c)-(d) the initial contour with a reduction = 5 and the extracted contour of segmentation of a malignant case.

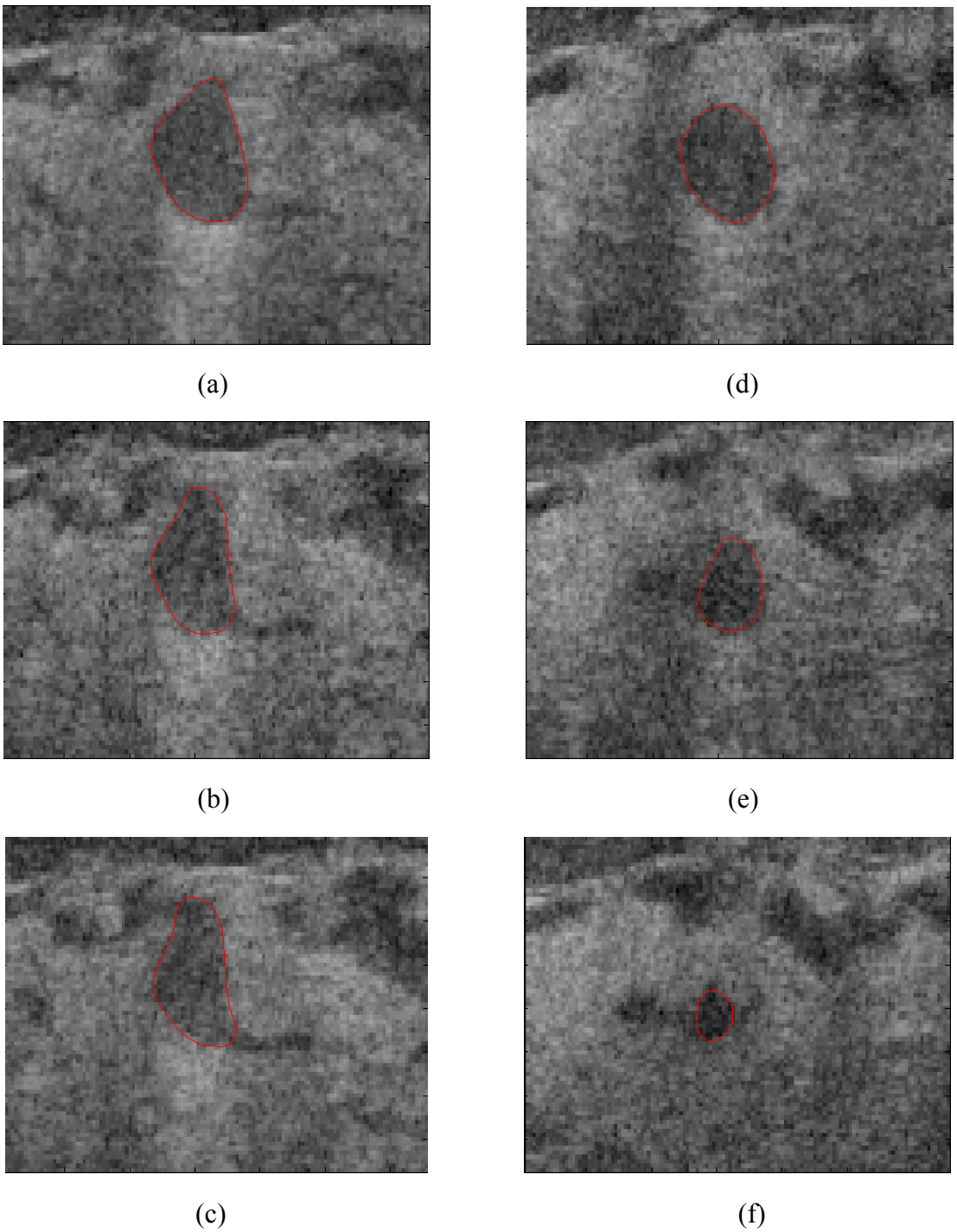

Fig. 11. Result of contour segmentation (benign case): (a)-(c) were contours in the preceding slices, and (d)-(f) were contours in the following slices.

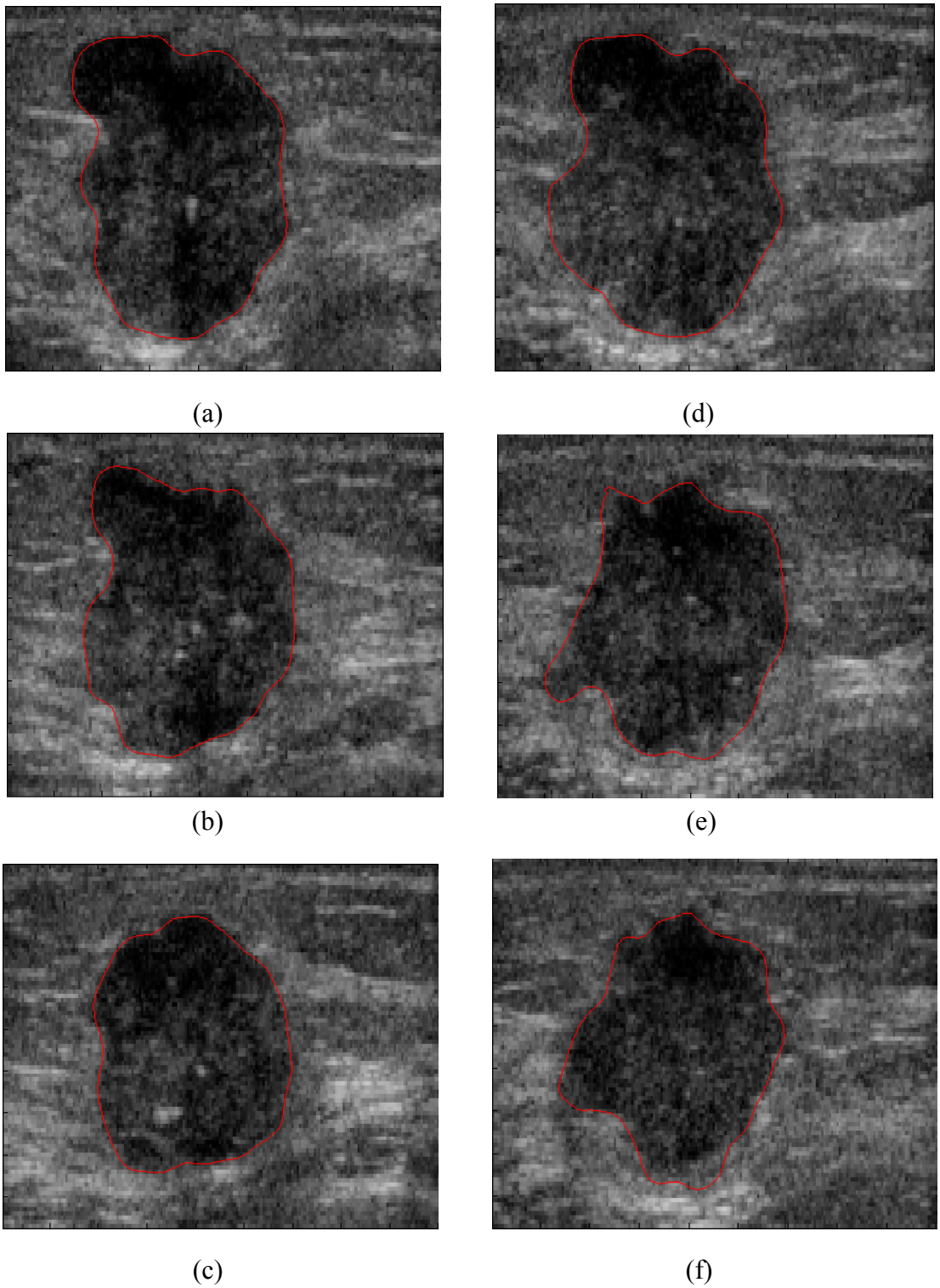

Fig. 12. Result of contour segmentation (malignant case): (a)-(c) were contours in the preceding slices, and (d)-(f) were contours in the following slices.

Table 3. The A*z* values and standard deviations of the 11 features including vascular features, patients' age, and volume of VOI in the proposed CAD system with contouring method and the previous CAD system. (154 cases)

	CAD with automatic contouring method		**CAD**	
Feature	A*z*	std	Az	std
VI_E	0.7407	0.0406	0.7500	0.0425
VI_{VOI}	0.6714	0.0431	0.6663	0.0453
VI_O	0.7658	0.0386	0.7760	0.0397
FI_E	0.6980	0.0406	0.6894	0.0424
FI_{VOI}	0.6416	0.0428	0.6314	0.0445
FI_O	0.6931	0.0407	0.6812	0.0428
VFI_E	0.7733	0.0390	0.7696	0.0412
VFI_{VOI}	0.6789	0.0428	0.6718	0.0449
VFI_O	0.7760	0.0387	0.7850	0.0397
Volume of VOI	0.8138	0.0328	0.8263	0.0326
Patients' age	0.7940	0.0344	0.7862	0.0360

std: standard deviation

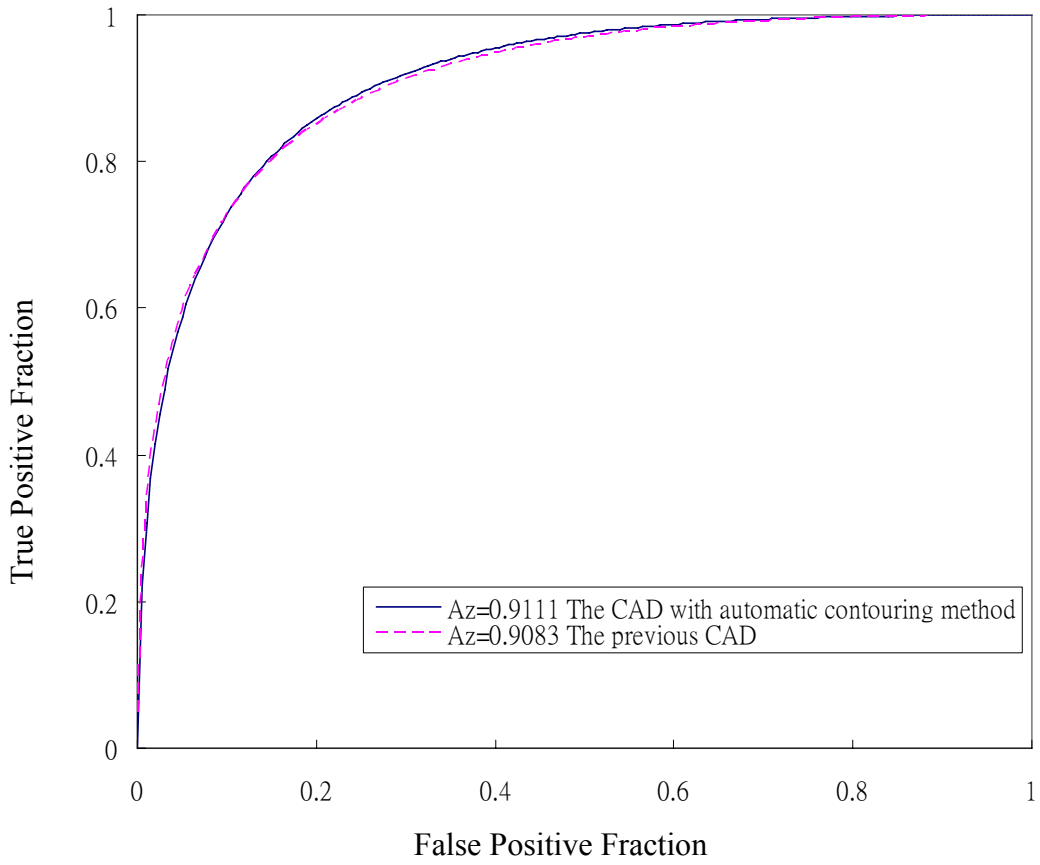

Fig. 13. Receiver operating characteristic (ROC) analysis of the proposed CAD system with automatic contouring method and the previous CAD system with the entire feature sets.

CHAPTER 4

CONCLUSION

This study proposed a CAD system to evaluate the diagnostic results of 3-D power Doppler ultrasound in classifying the breast tumors. 3-D power Doppler ultrasound enabled the detection and measurement of the vascularity within the entire volume of tumor. Besides, the patients' age and volume of VOI were considered in this study. The SVM model was employed to classify the breast tumors. Compared to neural networks, the training and diagnostic procedure of SVM is faster and more stable[31].

A total of 11 features including vascular features, patients' age, and volume of VOI were applied in the experiment. The SVM system classifies the breast tumors by utilized these features. The A*z* values and standard deviations of all features are present in Table 2. According to the results, the vascular features are useful in differencing benign and malignant breast tumors. The A*z* value of volume of VOI is 0.81 is the highest value in the experiment. The volume of VOI can rough represent the tumor's size which is an important feature to physician. In addition, the most-distinguishing feature of the results is patients' age. The mean age of all patients was 44 and the age range was 17-80 years. Furthermore, the mean age was 51 (range 32-80 years) years for the patients with malignant breast tumor and 39 (range 17-72 years) years for the benign group. The likelihood of breast cancer in patient over 44 years was 68% (52/77) and the

A*z* value of patients' age was 0.79. The patients' age was seldom considered to be a feature in the past, but it was valuable to this study.

In the proposed CAD system with automatic contouring method in chapter 3, an effective contouring method was applied in this study. After the image preprocessing, the segmentation results from the proposed method were precision. Only a small number of cases might segmentation unsuccessfully. The proposed CAD system with contouring method evaluated volumes of tumors and vascular features to distinguish between benign and malignant lesions by using SVM. Comparing with the previous CAD system, the CAD system with contouring method obtained the better result. It says the CAD system with contouring method was effective and more accurately. However, the feature of volume of tumor in the CAD system with contouring method was inferior to the previous CAD system. The volume of tumor in the previous CAD system was just evaluated from VOI. Due to the malignant tumor usually have irregular shapes and anfractuous boundary, a malignant tumor frequently has a large region of ROI. The previous CAD system evaluates the volume of VOI directly is not really precision. And the volume of tumor in the CAD system with contouring method is more similar to the real size of tumor. Maybe we can evaluate the other features such as shape and boundary to improve the diagnostic accuracy in the future.

Beside, it is effective in classifying breast tumor according to these 11 features.

However, the anarchic vascularity of a malignant breast tumor is hard to command. Moreover, the vascularity in inner and outer volume of VOI is worth noticing. A recent study showed malignant tumors have higher vascularity than benign lesions both in tumor itself and surrounding the tumor[15]. Therefore, we desire to evaluate the intra and inter- power Doppler signal for a tumor in the future. In conclusion, the proposed method combining 3-D power Doppler vascularity with patients' age and volume of VOI has a good result of differentiating benign and malignant breast tumors by using SVM. Experimental investigations demonstrated that the vascular features of 3-D power Doppler were effective and the patients' age and volume of VOI is useful for differential diagnosis of breast tumors.

REFERENCES

[1] J. Folkman, "Tumor angiogenesis," *Adv. Cancer Res.*, vol. 43 pp. 175-203, 1985.

[2] J. Folkman, "What is the evidence that tumors are angiogenesis dependent?" *J. Natl. Cancer Inst.*, vol. 82, no. 1, pp. 4-6, Jan. 1990.

[3] Sehgal CM, Arger PH, and Rowling SE, "Quantitative vascularity of breast masses by Doppler imaging: regional variations and diagnostic implications," *Journal of Ultrasound in Medicine*, vol. 19, no. 7, pp. 427-440, 2000.

[4] D.O. Cosgrove, J.C. Bamber, J.B. Davey, J.A. McKinna, and H.D. Sinnett, "Color Doppler signals from breast tumors. Work in progress," *Radiology*, vol. 176, no. 1, pp. 175-180, July 1990.

[5] M.M. McNicholas, P.M. Mercer, J.C. Miller, E.W. McDermott, N.J. O'Higgins, and D.P. MacErlean, "Color Doppler sonography in the evaluation of palpable breast masses," *AJR Am. J. Roentgenol.*, vol. 161, no. 4, pp. 765-771, Oct. 1993.

[6] H. Madjar, W. Sauerbrei, H.J. Prompeler, R. Wolfarth, and H. Gufler, "Color Doppler and duplex flow analysis for classification of breast lesions," *Gynecol. Oncol.*, vol. 64, no. 3, pp. 392-403, Mar. 1997.

[7] H. Madjar, "Breast examinations with continuous wave and color Doppler," *Ultrasound Obstet. Gynecol.*, vol. 2, no. 3, pp. 215-220, May 1992.

[8] J.U. Blohmer, H. Oellinger, C. Schmidt, P. Hufnagl, R. Felix, and W. Lichtenegger, "Comparison of various imaging methods with particular evaluation of color Doppler sonography for planning surgery for breast tumors,"

Arch. Gynecol. Obstet., vol. 262, no. 3-4, pp. 159-171, 1999.

[9] Wright IA, Pugh ND, Lyons K, Webster DJ, and Mansel RE, "Power Doppler in breast tumours: a comparison with conventional colour Doppler imaging," *European Journal of Ultrasound*, vol. 7, no. 3, pp. 175-181, Aug. 1998.

[10] S.W. Lee, H.Y. Choi, S.Y. Baek, and S.M. Lim, "Role of color and power doppler imaging in differentiating between malignant and benign solid breast masses," *J. Clin. Ultrasound*, vol. 30, no. 8, pp. 459-464, Oct. 2002.

[11] Carson PL, Moskalik AP, Govil A, Roubidoux MA, Fowlkes JB, Normolle D et al., "The 3D and 2D color flow display of breast masses," *Ultrasound in Medicine and Biology*, vol. 23, no. 6, pp. 837-849, 1997.

[12] Chang RF, Huang SF, Moon WK, Lee YH, and Chen DR, "Computer algorithm for analysing breast tumor angiogenesis using 3-D power Doppler ultrasound," *Ultrasound in Medicine and Biology*, vol. 32, no. 10, pp. 1499-1508, Oct. 2006.

[13] Riccabona M, Nelson TR, and Pretorius DH, "Three-dimensional ultrasound: Accuracy of distance and volume measures," *Ultrasound in Obstetrics and Gynecology*, vol. 7, no. 6, pp. 429-434, June 1996.

[14] Chen DR, Chang RF, Wu WJ, Moon WK, and Wu WL, "3-D breast ultrasound segmentation using active contour model," *Ultrasound in Medicine and Biology*, vol. 29, no. 7, pp. 1017-1026, July 2003.

[15] Hsiao YH, Kuo SJ, Liang WM, Huang YL, and Chen DR, "Intra-Tumor Flow Index Can Predict the Malignant Potential of Breast Tumor: Dependent on Age

and Volume," *Ultrasound in Medicine and Biology*, 2007.

[16] "Breast Cancer Facts and Figures 2003-2004.," *American Cancer Society*, 2005.

[17] Christianini N and Shawe-Taylor J, *An Introduction to Support Vector Machines and Other Kernel-Based Learning Methods* United Kingdom: Cambridge University Press, 2000.

[18] Song Q, Hu WJ, and Xie WF, "Robust support vector machine with bullet hole image classification," *IEEE Transactions on Systems Man and Cybernetics Part C: Applications and Reviews*, vol. 32, no. 4, pp. 440-448, Nov. 2002.

[19] Kim KI, Jung K, Park SH, and Kim HJ, "Support vector machines for texture classification," *IEEE Transactions on Pattern Analysis and Machine Intelligence*, vol. 24 pp. 1542-1550, 2002.

[20] Yang MH, Roth D, and Ahuja N, "A tale of two classifiers: SNoW vs. SVM in visual recognition," *European Conference on Computer Vision*, vol. 2353 pp. 685-699, 2002.

[21] Song MH, Breneman CM, Bi JB, Sukumar N, Bennett KP, Cramer S et al., "Prediction of protein retention times in anion-exchange chromatography systems using support vector regression," *Journal of Chemical Information and Computer Sciences*, vol. 42 pp. 1347-1357, 2002.

[22] El Naqa I, Yang YY, Wernick MN, Galatsanos NP, and Nishikawa RM, "A support vector machine approach for detection of microcalcifications," *IEEE*

Transactions on Medical Imaging, vol. 21, no. 12, pp. 1552-1563, Dec. 2002.

[23] Sun YF, Fan XD, and Li YD, "Identifying splicing sites in eukaryotic RNA: support vector machine approach," *Computers in Biology and Medicine*, vol. 33 pp. 17-29, 2003.

[24] Chen DR, Chang RF, Chen WM, and Moon WK, "Computer-Aided Diagnosis for 3-Dimensional Breast Ultrasonography," *Archives of Surgery*, vol. 138 pp. 296-302, 2003.

[25] Jarvela IY, Sladkevicius P, Kelly S, Ojha K, Nargund G, and Campbell S, "Three-dimensional sonographic and power Doppler characterization of ovaries in late follicular phase," *Ultrasound in Obstetrics and Gynecology*, vol. 20 pp. 281-285, 2002.

[26] Vapnik V, *Staistical Learning Theory* New York: John Wiley & Sons, 1998.

[27] J.S. Lim, "Two-Dimensional Signal and Image Processing," *Englewood Cliffs, NJ:Prentice Hall*, pp. 536-540, 1990.

[28] R. Sharma and B. D. Van Veen, "Large modular structures for adaptive beamformering and the Gram–Schmidt preprocessor," *IEEE Trans. Signal Processing*, vol. 42, pp. 448–451, Feb. 1994.

[29] Y. L. Huang, Y. R. Jiang, D. R. Chen and W. K. Moon, "Level set segmentation for breast tumor in 2-D sonography," *Journal of Digital Imaging*, vol.20, no.3, pp.238-247, Sep. 2007.

[30] Cates JE, Lefohn AE, and Whitaker RT, "GIST: an interactive, GPU-based level set segmentation tool for 3D medical images," *Med.Image Anal*, vol.8, no. 3, pp. 217-231, 2004.

[31] Huang YL, Wang KL, and Chen DR, "Diagnosis of Breast Tumors with Ultrasonic Texture Analysis Using Support Vector Machines," *Neural Computing and Applications*, vol. 15, no. 2, pp. 164-169, Apr. 2006.